

Article

# The Influence of Liquid on the Outcome of Halogen-Bonded Metal–Organic Materials Synthesis by Liquid Assisted Grinding

Katarina Lisac and Dominik Cinčić \* 

Department of Chemistry, Faculty of Science, University of Zagreb, Horvatovac 102a, HR-10000 Zagreb, Croatia; katarina.lisac@chem.pmf.hr

\* Correspondence: dominik@chem.pmf.hr; Tel.: +385-1460-6362

Academic Editor: Franziska Emmerling

Received: 15 November 2017; Accepted: 4 December 2017; Published: 7 December 2017

**Abstract:** In this work, we describe novel multi-component halogen bonded solids of Co(II) complexes and 1,4-diodotetrafluorobenzene, **14tfib**. We present the important influence of liquid on the outcome of liquid assisted grinding of dichlorobis(1,10-phenantroline)cobalt(II),  $\text{CoCl}_2(\text{phen})_2$  and **14tfib**. Grinding of solid reactants with a small amount of water gives the cocrystal product  $[\text{CoCl}_2(\text{phen})_2](\text{14tfib})$  (**1**) while grinding with a small amount of methanol gives an ionic structure, the four-component solid  $[\text{CoCl}(\text{MeOH})(\text{phen})_2]\text{Cl}(\text{14tfib})(\text{MeOH})$  (**2**). Both solid products were also obtained by crystallization from the solution. Single crystal X-ray diffraction reveals that the dominant supramolecular interaction in **1** is the  $\text{I}\cdots\text{Cl}$  halogen bond between **14tfib** and  $\text{CoCl}_2(\text{phen})_2$  building blocks. On the other hand, the dominant supramolecular interactions in **2** are  $\text{I}\cdots\text{Cl}^-$  charge-assisted halogen bonds between the halogen bond donor and the chloride anion as well as hydrogen bonds between the chloride anion and OH groups of coordinated and solvated methanol molecules.

**Keywords:** liquid assisted grinding; cocrystals; halogen bonding; ionic cocrystals; charge assisted halogen bond

## 1. Introduction

The study of multi-component materials, e.g., cocrystals and salts, has become one of the most attractive areas of research in the field of solid-state chemistry [1]. Effective synthesis of such materials utilizes appropriate molecular building blocks, either neutral or ionic, and supramolecular interactions which lead to reliable motifs of molecular assembly [2,3]. Over the past two decades, halogen bond [4] has been recognized as a reliable crystal engineering tool [5]. It is an attractive interaction between a positively charged area of a covalently bound halogen atoms (Br, I) and Lewis bases (nucleophilic atoms such as O, N, S, etc.) [6,7]. Typical halogen bonds are similar to hydrogen bonds in terms of both length and directionality [8,9]. Their strength strongly depends on the surroundings to which the halogen atom is bonded and on acceptor atom basicity [10,11].

The use of halogen bonding in crystal engineering of metal–organic materials remains a persistent challenge pursued by several groups [12–16]. Several reports and reviews have been published dealing with halogen bonding in crystal engineering of single component metal–organic solids [12,13]. In contrast, synthesis of multi-component metal–organic materials with halogen bond donors has received much less attention. In such materials, metal–organic building blocks can be employed in several different ways as halogen bond acceptors. Most reports have focused on the formation of ionic structures involving complexes of simple inorganic ligands (e.g.,  $\text{Cl}^-$ ,  $\text{CN}^-$ , etc.) [17–19]. On the other hand, much less explored systems, recently introduced, are neutral metal–organic cocrystals

where coordination compounds are building blocks which contain ligands with pendant halogen bond acceptors group [20–22].

Herein, following previous studies on halogen-bonded cocrystal syntheses with neutral metal–organic electron donor units which contain simple inorganic ligands ( $\text{Cl}^-$ ) [12,17], and to explore the halogen bonding proclivity of the chlorine atom coordinated to metal, we report the synthesis of multi-component solids derived from dichlorobis(1,10-phenanthroline)cobalt(II), ( $\text{CoCl}_2(\text{phen})_2$ ), and a commonly used halogen bond donor, 1,4-diiodotetrafluorobenzene, (**14tfib**) (Figure 1). The complex  $\text{CoCl}_2(\text{phen})_2$  is stable in solution and can be easily prepared by reacting  $\text{CoCl}_2(\text{H}_2\text{O})_6$  with two equivalents of **phen** in various solvents, e.g., methanol, ethanol, acetonitrile, etc. [23,24]. Over the past several decades, **phen** has been used as a versatile reagent for analytical, inorganic and supramolecular chemistry, and numerous **phen** coordination compounds have been reported [25,26]. A survey of the Cambridge Structural Database (CSD; version 5.38) [27] based on **phen** complexes with transition metals ( $\text{MCl}_2(\text{phen})_n$  units) has resulted in 70 hits. Restraining the search further, to Co complexes, has resulted in 17 hits. Of those, 15 structures correspond to salts, solvates or hydrates of  $\text{CoCl}_2(\text{phen})_2$  and there are no entries corresponding to halogen bonded cocrystals. Furthermore, even though halogen atoms bonded to metal centers are potent as halogen bond acceptors, a survey based on the ability of any transition metal complexes, of the  $\text{MX}_n\text{L}_m$  type (X = halogen atom; L = any organic ligands) to act as a halogen bond acceptor with haloperfluorinated benzenes as halogen bond donors, via  $\text{M-X}\cdots\text{X}$  halogen bond, has resulted in only five hits.

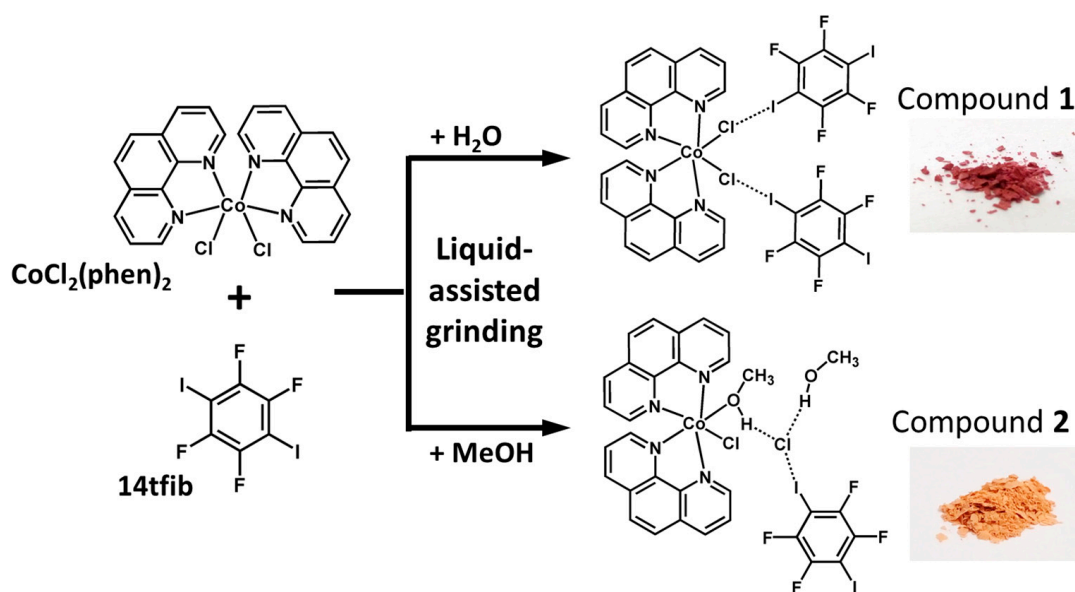


**Figure 1.** Mechanochemical synthesis of a halogen-bonded metal–organic structures: diagrams of **14tfib** and the  $\text{CoCl}_2(\text{phen})_2$  complex, and fragments of crystal structures of the resulting halogen-bonded metal–organic solids.

As the complex  $\text{CoCl}_2(\text{phen})_2$  is less soluble in organic solvents than the selected halogen bond donor, our cocrystal synthesis was based on mechanochemical liquid-assisted grinding (LAG), grinding of solid reactants in the presence of a small (catalytic) amount of liquid [28,29]. Throughout the last two decades, methods such as neat grinding (NG) and LAG have shown potential as efficient approaches for supramolecular and covalent synthesis applicable to a wide range of targets [30], including organic molecules, functional organic solids, organometallics, metal–organic materials, as well as inorganic materials [30–39]. In addition, LAG has been established as a fast and efficient screening method for desired crystal forms of molecular materials: for example, cocrystals, salts, solvates and polymorphs [40–43].

In the work presented herein, we describe the important role of liquid on the outcome of synthesis of halogen-bonded metal–organic materials by LAG. Grinding solid reactants with a small amount of water gives a two-component solid, the cocrystal product  $[\text{CoCl}_2(\text{phen})_2](\mathbf{14tfib})$  (compound **1**), while grinding with a small amount of methanol gives a four-component ionic solid, the salt of cocrystal solvate  $[\text{CoCl}(\text{MeOH})(\text{phen})_2]\text{Cl}(\mathbf{14tfib})(\text{MeOH})$  (compound **2**) (Figure 1). Both solid products were also obtained by crystallization from the solution and characterized by single crystal X-ray diffraction. To the best of our knowledge, we report the first known cocrystal of neutral  $\text{CoCl}_2(\text{phen})_2$  building block with a  $\text{I}\cdots\text{Cl}\cdots\text{M}$  halogen bond motif, as well as the first known ionic multi component solid of **14tfib** containing a cobalt complex cation, with a  $\text{I}\cdots\text{Cl}^-$  charge-assisted halogen bond.

## 2. Results and Discussion

### 2.1. Syntheses

As the solid-state synthesis of halogen bonded cocrystals has been described in earlier studies [44–47], we have decided to attempt to synthesize the targeted cocrystals by LAG. All reactants and products have been characterized by means of powder X-ray diffraction (PXRD) (Figures S1 and S2) and thermogravimetry analysis (TGA). We first attempted grinding solid reactants,  $\text{CoCl}_2(\text{phen})_2$  and **14tfib**, in the 1:1 stoichiometric ratio and in the presence of a small amount of methanol. The PXRD pattern of the orange solid product obtained after 60 min grinding, was measured and compared with powder patterns of reactants, and has shown that the obtained solid was a new phase (Figure 2). To observe the grinding experiment, as well as to produce single crystal suitable for X-ray diffraction experiment, we have performed the reaction from the methanol solution. Single crystal X-ray diffraction reveals that we obtained a methanol solvate of an ionic cocrystal, **2**, which consists of  $\text{CoCl}(\text{phen})_2(\text{MeOH})$  cation units, a chloride anion and **14tfib**. PXRD pattern calculated from the obtained single crystal data was in good agreement with the diffraction pattern measured on the bulk material obtained by LAG (Figure 2). Repeating the synthesis by LAG of solid reactants, also in the 1:1 stoichiometric ratio and in the presence of a small amount of water, we obtained a new phase, a red solid product, its PXRD pattern different from that of **2**. Furthermore, through synthesis from a mixture of dichloromethane and ethanol, we obtained crystals of identical PXRD as that of the product obtained by LAG in the presence of water. Single crystal X-ray diffraction revealed that this time we obtained the cocrystal of  $\text{CoCl}_2(\text{phen})_2$  and **14tfib**, **1** (Figure 2).

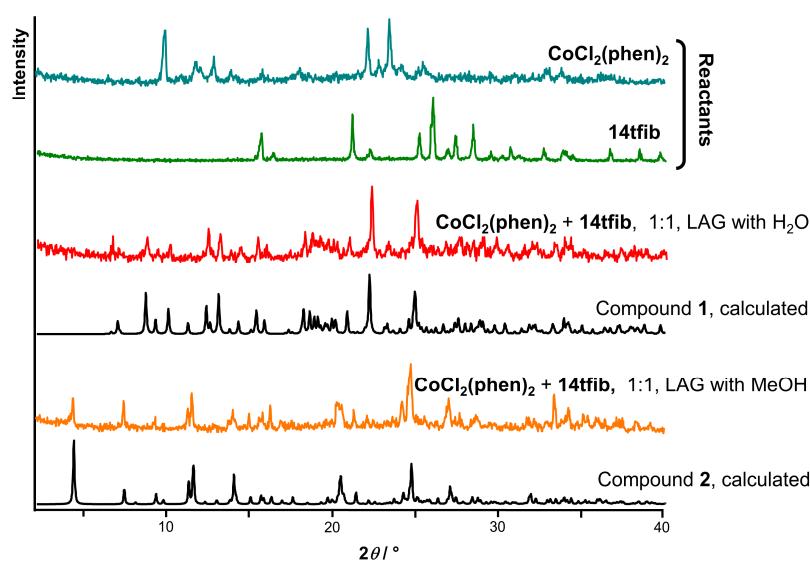


**Figure 2.** A comparison of the powder diffraction patterns of reactants, LAG products and diffraction patterns calculated from the obtained single crystal data of **1** and **2**.

TGA experiments show remarkably different thermal properties of the two prepared compounds (Figure 3). The TGA curve of **1** presents no obvious weight loss from 25 to 185 °C. In the range between 185 °C and 264 °C, a mass loss of 37% can be attributed to decomposition of the cocrystal. On the other hand, the TGA curve of **2** shows the start of decomposition at 123 °C (Figure 3). In the range between 123 °C and 178 °C, a mass loss of 7.8% can be attributed to decomposition of the complex due to the loss of methanol, both coordinated and solvated (calc. 6.7%). The second step is the same as for **1** and starts at 185 °C with a weight loss of 37% up to 185 °C. Annealing of **2** at 179 °C for 1 min promoted the formation of a red powder. Its PXRD pattern matched with that of **1** (see ESI, Figure S3). At room temperature, the reverse reaction could be achieved in the solid state by exposing **1** to methanol vapor for 16 h which yielded **2** (see ESI, Figure S4).

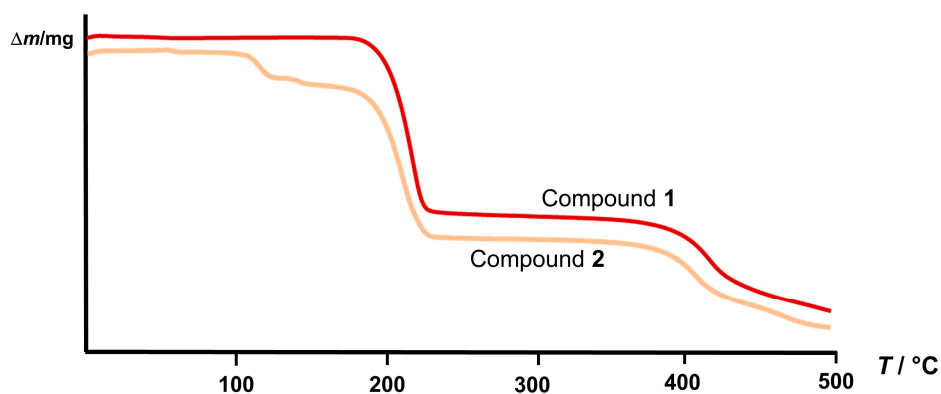


Figure 3. A comparison of the TG curves of **1** and **2**.

## 2.2. Structural Analysis

Molecular and crystal structure determination of the obtained single crystals revealed that we obtained solids containing different metal–organic building blocks which formed remarkably different supramolecular architecture in combination with **14tfib** (Figure 4). Compound **1** is a two-component solid, which consists of a neutral Co(II) complex and **14tfib**, while **2** is a four-component solid, in which Co(II) complex cations are the charge-balancing counterpart within halogen bond chains formed from Cl<sup>−</sup> and **14tfib**. General and crystallographic data for both compounds are given in Table 1.

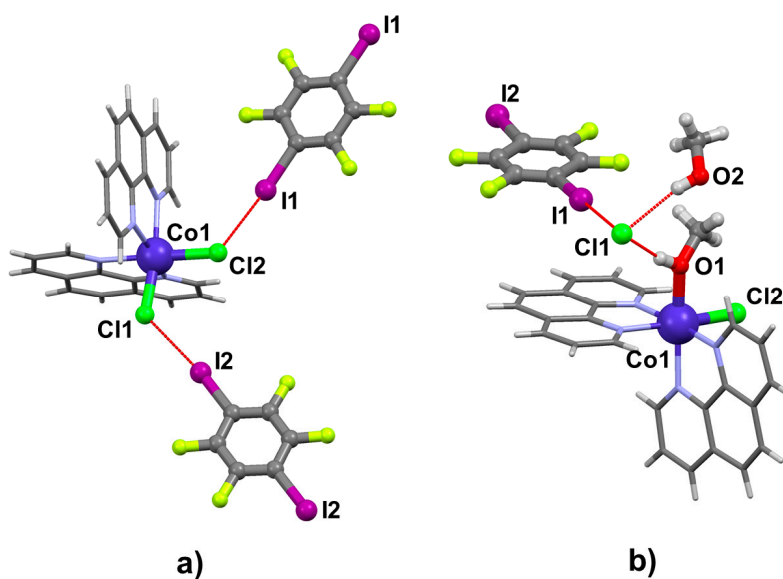
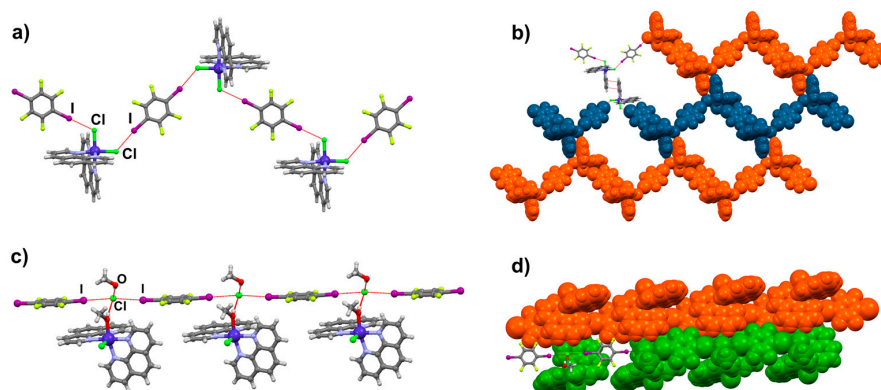


Figure 4. Structure of: (a) compound **1**; and (b) compound **2**.

**Table 1.** General and crystallographic data for the prepared compounds.

	Compound 1	Compound 2
<b>Molecular Formula</b>	<b>(CoCl<sub>2</sub>C<sub>24</sub>H<sub>16</sub>N<sub>4</sub>)(C<sub>6</sub>F<sub>4</sub>I<sub>2</sub>)</b>	<b>[(CoClC<sub>25</sub>H<sub>20</sub>N<sub>4</sub>O)]Cl(CH<sub>3</sub>OH)(C<sub>6</sub>F<sub>4</sub>I<sub>2</sub>)</b>
<i>M<sub>r</sub></i>	892.10	956.18
Crystal system	triclinic	triclinic
Space group	<i>P</i> $\bar{1}$	<i>P</i> $\bar{1}$
Crystal data:		
<i>a</i> /Å	9.9129(5)	9.1111(3)
<i>b</i> /Å	12.8302(5)	11.1583(5)
<i>c</i> /Å	14.0185(6)	17.8104(8)
$\alpha$ /°	116.357(4)	77.661(4)
$\beta$ /°	103.424(4)	76.942(4)
$\gamma$ /°	96.119(4)	81.311(3)
<i>V</i> /Å <sup>3</sup>	1508.31(13)	1713.04(13)
<i>Z</i>	2	2
<i>D</i> <sub>calc</sub> /g cm <sup>-3</sup>	1.964	1.854
$\lambda$ (MoK $\alpha$ )/Å	0.71073	0.71073
<i>T</i> /K	295	295
Crystal size/mm <sup>3</sup>	0.46 × 0.25 × 0.11	0.60 × 0.55 × 0.31
$\mu$ /mm <sup>-1</sup>	2.846	2.517
<i>F</i> (000)	854	926
Refl. collected/unique	6632/4212	5872/4242
Parameters	388	430
$\Delta\rho_{\max}$ , $\Delta\rho_{\min}$ /e Å <sup>-3</sup>	0.547; -0.632	0.586; -0.449
<i>R</i> [ <i>F</i> <sup>2</sup> > 4 $\sigma$ ( <i>F</i> <sup>2</sup> )]	0.0294	0.0297
<i>wR</i> ( <i>F</i> <sup>2</sup> )	0.0772	0.0655
Goodness-of-fit, <i>S</i>	0.879	0.940

The asymmetric unit of **1** contains one molecule of CoCl<sub>2</sub>(**phen**)<sub>2</sub> and two symmetrically inequivalent halves of **14tfib** molecules. The molecular structure of the CoCl<sub>2</sub>(**phen**)<sub>2</sub> unit is in a good agreement with that of the reported pure complex [23,24]. The Co(II) atom is coordinated by four N atoms from two **phen** molecules and two Cl atoms, forming a structure of distorted octahedral geometry with the following geometrical parameters: *d*(Co–N), ranging from 2.121 Å to 2.222 Å, *d*(Co1–Cl1) = 2.426 Å, *d*(Co1–Cl2) = 2.392 Å,  $\angle$ (N2–Co1–Cl1) = 97.0° and 87.4° between N–Co–N planes. In the crystal structure, each CoCl<sub>2</sub>(**phen**)<sub>2</sub> unit is connected with **14tfib** via I⋯Cl halogen bonds (*d*(I2⋯Cl1) = 3.145 Å,  $\angle$ (C–I⋯Cl) = 172.9°; *d*(I1⋯Cl2) = 3.137 Å,  $\angle$ (C–I⋯Cl) = 169.7°) leading to the formation of zig-zag chains (Figure 5a, Table S1). The chains are connected into layers via contacts between aromatic rings of adjacent molecules (*d*(C15⋯C16) = 3.387 Å) and form layers (Figure 5b) which are further connected into a 3D network by two types of C–H⋯I interactions between **14tfib** and **phen** (*d*(C8⋯I1) = 3.899 Å, *d*(C18⋯I2) = 3.808 Å).

**Figure 5.** Parts of the crystal structure of prepared solids: halogen bonded zig-zag chain (a) and 2D network (b) of **1**; and halogen bonded chain (c) and 2D network (d) of **2**.

The asymmetric unit of **2** contains the  $[\text{CoCl}(\text{MeOH})(\text{phen})_2]^+$  cation complex, a  $\text{Cl}^-$  anion, a MeOH molecule and a **14tfib** molecule. The molecular structure of the  $[\text{CoCl}(\text{MeOH})(\text{phen})_2]^+$  cation is similar to  $\text{CoCl}_2(\text{phen})_2$ , where one Cl atom is substituted with a coordinated MeOH molecule. The Co(II) atom is coordinated by four N atoms from two **phen** molecules, one Cl atom, and one MeOH molecule forming a structure of distorted octahedral geometry with the following geometrical parameters:  $d(\text{Co}-\text{N})$  range from 2.121 Å to 2.145 Å,  $d(\text{Co1}-\text{Cl2}) = 2.416$  Å,  $d(\text{Co1}-\text{O1}) = 2.110$  Å,  $\angle(\text{N1}-\text{Co1}-\text{Cl2}) = 93.4^\circ$  and  $87.9^\circ$  between N–Co–N planes. In the crystal structure, dominant supramolecular interactions are  $\text{I}\cdots\text{Cl}^-$  charge-assisted halogen bonds between **14tfib** and the  $\text{Cl}^-$  anion ( $d(\text{I1}\cdots\text{Cl1}^-) = 3.159$  Å,  $\angle(\text{C}-\text{I}\cdots\text{Cl}^-) = 178.5^\circ$ ;  $d(\text{I2}\cdots\text{Cl1}^-) = 3.163$  Å,  $\angle(\text{C}-\text{I}\cdots\text{Cl}^-) = 176.1^\circ$ ) leading to the formation of chains (Figure 5c, Table S1). Since the  $\text{Cl}^-$  anion is a superior acceptor for both halogen and hydrogen bonds [48], the coordinated Cl atom acts only as an acceptor for weak  $\text{C}-\text{H}\cdots\text{Cl}$  hydrogen bonds ( $d(\text{C14}\cdots\text{Cl2}) = 3.657$  Å,  $d(\text{C20}\cdots\text{Cl2}) = 3.635$  Å). In the crystal structure, each  $\text{Cl}^-$  anion is connected with two **14tfib** molecules via the described halogen bonds, with a solvent MeOH molecule and with a cation complex (over the coordinated MeOH molecule) via  $\text{O}-\text{H}\cdots\text{Cl}^-$  hydrogen bonds ( $d(\text{O1}\cdots\text{Cl1}^-) = 3.029$  Å,  $d(\text{O2}\cdots\text{Cl1}^-) = 3.199$  Å) and with another cation complex via  $\text{C}-\text{H}\cdots\text{Cl}^-$  hydrogen bond ( $d(\text{C8}\cdots\text{Cl1}^-) = 3.784$  Å) (Table S2). Similar replacement of coordinated halide with a hydrogen donating solvent molecule, placing the halide in the second coordination sphere of the cation has already been described in bis(morpholine)diketonate Cu(II) compounds [49]. Formed halogen bonded chains (Figure 5c) are connected into layers via  $\text{C}-\text{H}\cdots\text{Cl}$ ,  $\text{C}-\text{H}\cdots\text{Cl}^-$  and  $\text{C}-\text{H}\cdots\text{F}$  interactions. Layers are further connected into a 3D network via  $\text{C}-\text{H}\cdots\text{C}$  and  $\text{C}\cdots\text{C}$  contacts (Figure 5d). The described charge-assisted halogen bond supramolecular motif has been recognized in earlier studies [50–52]. However, even though halide ( $\text{Cl}^-$ ,  $\text{Br}^-$ ,  $\text{I}^-$ ) anions are potent halogen bond acceptors, a survey of the CSD based on **14tfib** cocrystals with the  $\text{I}\cdots\text{X}^-$  motif has resulted in only 26 hits.

### 3. Materials and Methods

#### 3.1. Synthesis of Complexes

A mixture of 1.876 g (7.88 mmol)  $\text{CoCl}_2(\text{H}_2\text{O})_6$  and 3.125 g (15.76 mmol) **phen** was partially dissolved in 70.0 mL EtOH and refluxed with stirring for 3 h. The obtained red solid was filtered after one day.

#### 3.2. Mechanochemical Synthesis of **1**

A mixture of 40.0 mg (0.082 mmol)  $\text{CoCl}_2(\text{phen})_2$  and 32.9 mg (0.082 mmol) **14tfib** was placed in a 5 mL stainless steel jar along with 20  $\mu\text{L}$  of water and two stainless steel balls 5 mm in diameter. The mixture was then milled for 60 min in a Retsch MM200 Shaker Mill operating at 25 Hz frequency.

#### 3.3. Mechanochemical Synthesis of **2**

A mixture of 40.0 mg (0.082 mmol)  $\text{CoCl}_2(\text{phen})_2$  and 32.9 mg (0.082 mmol) **14tfib** was placed in a 5 mL stainless steel jar along with 20  $\mu\text{L}$  of methanol and two stainless steel balls 5 mm in diameter. The mixture was then milled for 60 min in a Retsch MM200 Shaker Mill operating at 25 Hz frequency.

#### 3.4. Crystallization of **1** and **2**

The single crystal of **1** was obtained by diffusion crystallization. A solution of **14tfib** (202.95 mg, 0.505 mmol) in 4.0 mL of dichloromethane was layered by a solution of  $\text{CoCl}_2(\text{H}_2\text{O})_6$  (30.0 mg, 0.126 mmol) and **phen** (50.0 mg, 0.252 mmol) in 5.0 mL of ethanol. The vial was stoppered and left at room temperature for a month.

The single crystal of **2** was obtained by dissolving a mixture of  $\text{CoCl}_2(\text{phen})_2$  (30.0 mg, 0.0612 mmol) and **14tfib** (68.7 mg, 0.171 mmol) in 4.0 mL of hot methanol and the subsequent cooling and solvent evaporation at room temperature for 2 days.

### 3.5. Thermal Analysis

TG measurements were performed on a Mettler-Toledo TGA/SDTA 851<sup>e</sup> module (Mettler-Toledo GmbH, Greifensee, Switzerland). Samples were placed in sealed 40  $\mu\text{L}$  aluminum pans with three pinholes and heated from 25 to 500  $^{\circ}\text{C}$  at a rate of 10  $^{\circ}\text{C min}^{-1}$  under nitrogen flow of 150  $\text{mL min}^{-1}$ . Data collection and analysis were performed using the program package STARe Software v14.00 [53].

### 3.6. Single Crystal X-ray Diffraction Experiments

The crystal and molecular structures of the prepared samples were determined by single crystal X-ray diffraction. Details of data collection and crystal structure refinement are listed in Table 1. Thermal ellipsoid plots showing the atom-labelling schemes are given in ESI (Figures S5 and S6). The diffraction data for **1** and **2** were collected at 295 K. Diffraction measurements were made on an Oxford Diffraction Xcalibur Kappa CCD X-ray diffractometer (Oxford Diffraction, Oxford, UK) with graphite-monochromated  $\text{MoK}\alpha$  ( $\lambda = 0.71073 \text{ \AA}$ ) radiation. The datasets were collected using the  $\omega$  scan mode over the  $2\theta$  range up to  $54^{\circ}$ . Programs CrysAlis CCD and CrysAlis RED were employed for data collection, cell refinement, and data reduction [54]. The structures were solved by direct methods and refined using the SHELXS, SHELXT and SHELXL programs, respectively [55,56]. The structural refinement was performed on  $F^2$  using all data. The hydrogen atoms not involved in hydrogen bonding were placed in calculated positions and treated as riding on their parent atoms [ $d(\text{C}-\text{H}) = 0.93 \text{ \AA}$  and  $U_{\text{iso}}(\text{H}) = 1.2 U_{\text{eq}}(\text{C})$ ] while the others were located from the electron difference map. All calculations were performed using the WINGX crystallographic suite of programs [57]. The molecular structures of compounds are presented by ORTEP-3 [57], and their molecular packing projections were prepared by Mercury [58].

### 3.7. Powder X-ray Diffraction Experiments

PXRD experiments on the samples were performed on a PHILIPS PW 1840 X-ray diffractometer (Philips Analytical B. V., Almelo, The Netherlands) with  $\text{CuK}\alpha_1$  ( $1.54056 \text{ \AA}$ ) radiation at 40 mA and 40 kV. The scattered intensities were measured with a scintillation counter. The angular range was from 3 to  $40^{\circ}$  ( $2\theta$ ) with steps of  $0.02\text{--}0.03^{\circ}$ , and the measuring time was  $0.2\text{--}0.5 \text{ s}$  per step. Data collection and analysis was performed using the program package Philips X'Pert [59–61].

## 4. Conclusions

To conclude, we have obtained two novel multi-component halogen bonded solids of  $\text{Co(II)}$  complexes by both liquid-assisted grinding and the conventional solvent-based method. We report the important role of liquid in directing the mechanochemical synthesis toward the intended solid product. Grinding of  $\text{CoCl}_2(\text{phen})_2$  complex and **14tfib** with a small amount of water gives the cocrystal product  $[\text{CoCl}_2(\text{phen})_2](\text{14tfib})$ , in which the dominant supramolecular interactions are  $\text{I}\cdots\text{Cl}$  halogen bonds. Grinding solid reactants with a small amount of methanol gives an ionic structure, the four-component solid,  $[\text{CoCl}(\text{MeOH})(\text{phen})_2]\text{Cl}(\text{14tfib})(\text{MeOH})$ , in which the dominant supramolecular interactions are  $\text{I}\cdots\text{Cl}^-$  charge-assisted halogen as well as hydrogen bonds. To the best of our knowledge, we report the first known cocrystal of neutral  $\text{CoCl}_2(\text{phen})_2$  building block with a  $\text{I}\cdots\text{Cl}-\text{M}$  halogen bond motif. The coordinated chlorine can indeed be used as a reliable halogen acceptor in engineering multi-component metal–organic solids. We believe that the use of such metal–organic halogen bond acceptors may offer a general route to metal–organic halogen-bonded cocrystals. We are currently exploring the halogen bonding ability of other  $\text{MCl}_2\text{L}_2$  building blocks with octahedrally coordinated  $\text{Co(II)}$  and  $\text{Ni(II)}$  metal centers.

**Supplementary Materials:** The following are available online at [www.mdpi.com/2073-4352/7/12/363/s1](http://www.mdpi.com/2073-4352/7/12/363/s1), Figure S1: PXRD patterns of: (a)  $\text{CoCl}_2(\text{phen})_2$ ; (b) **14tfib**; (c) **1** by LAG; and (d) calculated pattern from single crystal data of **1**, Figure S2: PXRD patterns of: (a)  $\text{CoCl}_2(\text{phen})_2$ ; (b) **14tfib**; (c) **2** obtained by LAG; and (d) calculated pattern from single crystal data of **2**, Figure S3: PXRD patterns of: (a) **2** obtained by LAG; (b) **2** after annealing at  $179^{\circ}\text{C}$ ; (c) calculated pattern from single crystal data of **2**; and (d) calculated pattern from

single crystal data of **1**, Figure S4: PXRD patterns of: (a) **1** obtained by LAG; (b) **1** after exposure to methanol vapor for 16 h; (c) calculated pattern from single crystal data of **2**; and (d) calculated pattern from single crystal data of **1**, Figure S5: Molecular structure of **1** showing the atom-labeling scheme. Displacement ellipsoids are drawn at the 50% probability level and H atoms are shown as small spheres of arbitrary radius, Figure S6: Molecular structure of **2** showing the atom-labeling scheme. Displacement ellipsoids are drawn at the 50% probability level and H atoms are shown as small spheres of arbitrary radius, Table S1: Geometric parameters for the halogen bonds in **1** and **2**, Table S2: Geometric parameters for the hydrogen bonds in **1** and **2**. CCDC 1585631 and 1585632 contain crystallographic data for this paper. These data can be obtained free of charge from the Director, CCDC, 12 Union Road, Cambridge, CBZ 1EZ, UK (Fax: +44-1223-336033; email: deposit@ccdc.cam.ac.uk or www: <http://www.ccdc.cam.ac.uk>).

**Acknowledgments:** This research was supported by the Croatian Science Foundation under the project IP-2014-09-7367. We are grateful to Vladimir Stilinović and Vinko Nemec for helpful suggestions.

**Author Contributions:** Katarina Lisac and Dominik Cinčić conceived and designed the experiments; Katarina Lisac performed the experiments; Katarina Lisac and Dominik Cinčić analyzed the data; Dominik Cinčić and Katarina Lisac contributed reagents/materials/analysis tools; Katarina Lisac and Dominik Cinčić wrote the paper.

**Conflicts of Interest:** There are no conflicts to declare.

## References

1. Desiraju, G.R. Crystal engineering: A holistic view. *Angew. Chem. Int. Ed.* **2007**, *46*, 8342–8356. [[CrossRef](#)] [[PubMed](#)]
2. Aakeröy, C.B.; Salmon, D.J. Building co-crystals with molecular sense and supramolecular sensibility. *CrystEngComm* **2005**, *7*, 439–448. [[CrossRef](#)]
3. Friščić, T. Supramolecular concepts and new techniques in mechanochemistry: Cocrystals, cages, rotaxanes, open metal–organic frameworks. *Chem. Soc. Rev.* **2012**, *41*, 3493–3510. [[CrossRef](#)] [[PubMed](#)]
4. Hassel, O. Structural aspects of interatomic charge-transfer bonding. *Science* **1970**, *170*, 497–502. [[CrossRef](#)] [[PubMed](#)]
5. Cavallo, G.; Metrangolo, P.; Milani, R.; Pilati, T.; Priimägi, A.; Resnati, G.; Terraneo, G. The Halogen Bond. *Chem. Rev.* **2016**, *116*, 2478–2601. [[CrossRef](#)] [[PubMed](#)]
6. Politzer, P.; Murray, J.S.; Clark, T. Halogen bonding: An electrostatically-driven highly directional noncovalent interaction. *Phys. Chem. Chem. Phys.* **2010**, *12*, 7748–7757. [[CrossRef](#)] [[PubMed](#)]
7. Priimägi, A.; Cavallo, G.; Metrangolo, P.; Resnati, G. The Halogen Bond in the Design of Functional Supramolecular Materials: Recent Advances. *Acc. Chem. Res.* **2013**, *46*, 2686–2695. [[CrossRef](#)] [[PubMed](#)]
8. Fourmigué, M. Halogen bonding: Recent advances. *Curr. Opin. Solid State Mater. Sci.* **2009**, *13*, 36–45. [[CrossRef](#)]
9. Cinčić, D.; Friščić, T.; Jones, W. Isostructural Materials Achieved by Using Structurally Equivalent Donors and Acceptors in Halogen-Bonded Cocrystals. *Chem. Eur. J.* **2008**, *14*, 747–753. [[CrossRef](#)] [[PubMed](#)]
10. Metrangolo, P.; Neukirch, H.; Pilati, T.; Resnati, G. Halogen Bonding Based Recognition Processes: A World Parallel to Hydrogen Bonding. *Acc. Chem. Res.* **2005**, *38*, 386–395. [[CrossRef](#)] [[PubMed](#)]
11. Stilinović, V.; Horvat, G.; Hrenar, T.; Nemec, V.; Cinčić, D. Halogen and Hydrogen Bonding between (N-Halogeno)-succinimides and Pyridine Derivatives in Solution, the Solid State and In Silico. *Chem. Eur. J.* **2017**, *22*, 5244–5257. [[CrossRef](#)] [[PubMed](#)]
12. Bertani, R.; Sgarbossa, P.; Venzo, A.; Lelj, F.; Amati, M.; Resnati, G.; Pilati, T.; Metrangolo, P.; Terraneo, G. Halogen bonding in metal–organic–supramolecular networks. *Coord. Chem. Rev.* **2010**, *254*, 677–695. [[CrossRef](#)]
13. Mahmudov, K.T.; Kopylovich, M.N.; Guedes da Silva, M.F.C.; Pombeiro, A.J.L. Non-covalent interactions in the synthesis of coordination compounds: Recent advances. *Coord. Chem. Rev.* **2017**, *345*, 54–72. [[CrossRef](#)]
14. Li, B.; Zhang, S.-Q.; Wang, L.-Y.; Mak, T.C.W. Halogen bonding: A powerful, emerging tool for constructing high-dimensional metal-containing supramolecular networks. *Coord. Chem. Rev.* **2016**, *308*, 1–21. [[CrossRef](#)]
15. Gamekkanda, J.C.; Sinha, A.S.; Desper, J.; Đaković, M.; Aakeröy, C.B. The Role of Halogen Bonding in Controlling Assembly and Organization of Cu (II)-Acac Based Coordination Complexes. *Crystals* **2017**, *7*, 226. [[CrossRef](#)]

16. Aakeröy, C.B.; Schultheiss, N.; Desper, J.; Moore, C. Attempted assembly of discrete coordination complexes into 1-D chains using halogen bonding or halogen···halogen interactions. *CrystEngComm* **2007**, *9*, 421–426. [[CrossRef](#)]
17. Johnson, M.T.; Džolić, Z.; Cetina, M.; Wendt, O.F.; Ohrstrom, L.; Rissanen, K. Neutral Organometallic Halogen Bond Acceptors: Halogen Bonding in Complexes of PCPPdX (X = Cl, Br, I) with Iodine (I<sub>2</sub>), 1,4-Diiodotetrafluorobenzene (F4DIBz), and 1,4-Diiodooctafluorobutane (F8DIBu). *Cryst. Growth Des.* **2012**, *12*, 362–368. [[CrossRef](#)] [[PubMed](#)]
18. Christopherson, J.-C.; Potts, K.P.; Bushuyev, O.S.; Topić, F.; Huskić, I.; Rissanen, K.; Barrett, C.J.; Friščić, T. Assembly and dichroism of a four-component halogen-bonded metal-organic cocrystal salt solvate involving dicyanoaurate(I) acceptors. *Faraday Discuss.* **2017**, *203*, 441–457. [[CrossRef](#)] [[PubMed](#)]
19. Ding, X.; Tuikka, M.J.; Hirva, P.; Kukushkin, V.Y.; Novikov, A.S.; Haukka, M. Fine-tuning halogen bonding properties of diiodine through halogen–halogen charge transfer—Extended [Ru(2,2′-bipyridine)(CO)<sub>2</sub>X<sub>2</sub>]<sub>2</sub>·I<sub>2</sub> systems (X = Cl, Br, I). *CrystEngComm* **2016**, *18*, 1987–1995. [[CrossRef](#)]
20. Cinčić, D.; Friščić, T. Synthesis of an extended halogen-bonded metal–organic structure in a one-pot mechanochemical reaction that combines covalent bonding, coordination chemistry and supramolecular synthesis. *CrystEngComm* **2014**, *16*, 10169–10172. [[CrossRef](#)]
21. Lapadula, G.; Judaš, N.; Friščić, T.; Jones, W. A Three-Component Modular Strategy to Extend and Link Coordination Complexes by Using Halogen Bonds to O, S and  $\pi$  Acceptors. *Chem. Eur. J.* **2010**, *16*, 7400–7403. [[CrossRef](#)] [[PubMed](#)]
22. Nemeč, V.; Fotović, L.; Friščić, T.; Cinčić, D. A Large Family of Halogen-Bonded Cocrystals Involving Metal–Organic Building Blocks with Open Coordination Sites. *Cryst. Growth Des.* **2017**. [[CrossRef](#)]
23. Chen, X.; Han, S.; Wang, R.; Li, Y. Four supramolecular isomers of dichloridobis(1,10-phenanthroline)cobalt(II): Synthesis, structure characterization and isomerization. *Acta Crystallogr. Sect. C* **2016**, *72*, 6–13. [[CrossRef](#)] [[PubMed](#)]
24. Li, L.-L.; Liu, D.-X.; Liu, T.-F. A polymorph of *cis*-dichloridobis(1,10-phenanthroline- $\kappa^2N,N'$ )cobalt(II). *Acta Crystallogr. Sect. E* **2007**, *63*, m1880. [[CrossRef](#)]
25. Moulton, B.; Zaworotko, M.J. From Molecules to Crystal Engineering: Supramolecular Isomerism and Polymorphism in Network Solids. *Chem. Rev.* **2001**, *101*, 1629–1658. [[CrossRef](#)] [[PubMed](#)]
26. Ye, B.; Tong, M.; Chen, X. Metal-organic molecular architectures with 2,2′-bipyridyl-like and carboxylate ligands. *Coord. Chem. Rev.* **2005**, *249*, 545–565. [[CrossRef](#)]
27. Groom, C.R.; Bruno, I.J.; Lightfoot, M.P.; Ward, S.C. The Cambridge Structural Database. *Acta Crystallogr. B* **2016**, *B72*, 171–179. [[CrossRef](#)] [[PubMed](#)]
28. Braga, D.; Curzi, M.; Johansson, A.; Polito, M.; Rubini, K.; Grepioni, F. Simple and Quantitative Mechanochemical Preparation of a Porous Crystalline Material Based on a 1D Coordination Network for Uptake of Small Molecules. *Angew. Chem. Int. Ed.* **2006**, *45*, 148–152. [[CrossRef](#)]
29. Friščić, T.; Childs, S.L.; Rizvi, S.A.A.; Jones, W. The role of solvent in mechanochemical and sonochemical cocrystal formation: A solubility-based approach for predicting cocrystallisation outcome. *CrystEngComm* **2009**, *11*, 418–426. [[CrossRef](#)]
30. James, S.L.; Adams, C.J.; Bolm, C.; Braga, D.; Collier, P.; Friščić, T.; Grepioni, F.; Harris, K.D.M.; Hyett, G.; Jones, W.; et al. Mechanochemistry: Opportunities for new and cleaner synthesis. *Chem. Soc. Rev.* **2012**, *41*, 413–447. [[CrossRef](#)] [[PubMed](#)]
31. Wang, G.-W. Mechanochemical organic synthesis. *Chem. Soc. Rev.* **2013**, *42*, 7668–7700. [[CrossRef](#)] [[PubMed](#)]
32. Friščić, T. New opportunities for materials synthesis using mechanochemistry. *J. Mater. Chem.* **2010**, *20*, 7599–7605. [[CrossRef](#)]
33. Braga, D.; Maini, L.; Grepioni, F. Mechanochemical preparation of co-crystals. *Chem. Soc. Rev.* **2013**, *42*, 7638–7648. [[CrossRef](#)] [[PubMed](#)]
34. Boldyreva, E.V. Mechanochemistry of inorganic and organic systems: What is similar, what is different? *Chem. Soc. Rev.* **2013**, *42*, 7719–7738. [[CrossRef](#)] [[PubMed](#)]
35. Cinčić, D.; Kaitner, B. Schiff base derived from 2-hydroxy-1-naphthaldehyde and liquid-assisted mechanochemical synthesis of its isostructural Cu(II) and Co(II) complexes. *CrystEngComm* **2011**, *13*, 4351–4357. [[CrossRef](#)]

36. Šepelák, V.; Düvel, A.; Wilkening, M.; Becker, K.-D.; Heitjans, P. Mechanochemical reactions and syntheses of oxides. *Chem. Soc. Rev.* **2013**, *42*, 7507–7520. [[CrossRef](#)] [[PubMed](#)]
37. Cinčić, D.; Brekalo, I.; Kaitner, B. Effect of atmosphere on solid-state amine-aldehyde condensations: Gas-phase catalysts for solid-state transformations. *Chem. Commun.* **2012**, *48*, 11683–11685. [[CrossRef](#)] [[PubMed](#)]
38. Cinčić, D.; Juribašić, M.; Babić, D.; Molčanov, K.; Šket, P.; Plavec, J.; Ćurić, M. New insight into solid-state molecular dynamics: Mechanochemical synthesis of azobenzene/triphenylphosphine palladacycles. *Chem. Commun.* **2011**, *47*, 11543–11545. [[CrossRef](#)] [[PubMed](#)]
39. Baláž, P.; Achimovičová, M.; Baláž, M.; Billik, P.; Cherkezova-Zheleva, Z.; Criado, J.M.; Delogu, F.; Dutková, E.; Gaffet, E.; José Gotor, F.; et al. Hallmarks of mechanochemistry: From nanoparticles to technology. *Chem. Soc. Rev.* **2013**, *42*, 7571–7637. [[CrossRef](#)] [[PubMed](#)]
40. Friščić, T.; Jones, W. Recent Advances in Understanding the Mechanism of Cocrystal Formation via Grinding. *Cryst. Growth Des.* **2009**, *9*, 1621–1637. [[CrossRef](#)]
41. Stilinović, V.; Cinčić, D.; Zbačnik, M.; Kaitner, B. Controlling solvate formation of a Schiff base by combining mechanochemistry with solution synthesis. *Croat. Chem. Acta* **2012**, *85*, 485–493. [[CrossRef](#)]
42. Braga, D.; Grepioni, F. Making crystals from crystals: A green route to crystal engineering and polymorphism. *Chem. Commun.* **2005**, 3635–3645. [[CrossRef](#)] [[PubMed](#)]
43. Springuel, G.; Robeyns, K.; Norberg, B.; Wouters, J.; Leyssens, T. Cocrystal Formation between Chiral Compounds: How Cocrystals Differ from Salts. *Cryst. Growth Des.* **2014**, *14*, 3996–4004. [[CrossRef](#)]
44. Cinčić, D.; Friščić, T.; Jones, W. A Stepwise Mechanism for the Mechanochemical Synthesis of Halogen-Bonded Cocrystal Architectures. *J. Am. Chem. Soc.* **2008**, *130*, 7524–7525. [[CrossRef](#)]
45. Cinčić, D.; Friščić, T.; Jones, W. Structural Equivalence of Br and I Halogen Bonds: A Route to Isostructural Materials with Controllable Properties. *Chem. Mater.* **2008**, *20*, 6623–6626. [[CrossRef](#)]
46. Mavračić, J.; Cinčić, D.; Kaitner, B. Halogen bonding of N-bromosuccinimide by grinding. *CrystEngComm* **2016**, *18*, 3343–3346. [[CrossRef](#)]
47. Nemeč, V.; Cinčić, D. Uncommon halogen bond motifs in cocrystals of aromatic amines and 1,4-diodotetrafluorobenzene. *CrystEngComm* **2016**, *18*, 7425–7429. [[CrossRef](#)]
48. Brammer, L.; Bruton, E.A.; Sherwood, P. Understanding the Behavior of Halogens as Hydrogen Bond Acceptors. *Cryst. Growth Des.* **2001**, *1*, 277–290. [[CrossRef](#)]
49. Stilinović, V.; Užarević, K.; Cvrtila, I.; Kaitner, B. Bis(morpholine) hydrogen bond pincer—A novel series of heteroleptic Cu(II) coordination compounds as receptors for electron rich guests. *CrystEngComm* **2012**, *14*, 7493–7501. [[CrossRef](#)]
50. Pfrunder, M.C.; Micallef, A.S.; Rintoul, L.; Arnold, D.P.; McMurtrie, J. Interplay between the Supramolecular Motifs of Polypyridyl Metal Complexes and Halogen Bond Networks in Cocrystals. *Cryst. Growth Des.* **2016**, *16*, 681–695. [[CrossRef](#)]
51. Cavallo, G.; Biella, S.; Lu, J.; Metrangolo, P.; Pilati, T.; Resnati, G.; Terraneo, G. Halide anion-templated assembly of di- and triiodoperfluorobenzenes into 2D and 3D supramolecular networks. *J. Fluor. Chem.* **2010**, *131*, 1165–1172. [[CrossRef](#)]
52. Raatikainen, K.; Rissanen, K. Modulation of N⋯I and +N–H⋯Cl⋯I Halogen Bonding: Folding, Inclusion, and Self-Assembly of Tri- and Tetraamino Piperazine Cyclophanes. *Cryst. Growth Des.* **2016**, *10*, 3638–3646. [[CrossRef](#)]
53. *STARe Software v.14.00*; MettlerToledo GmbH: Giessen, Germany, 2015.
54. Oxford Diffraction. *Xcalibur CCD System, CrysAlis CCD and CrysAlis RED*, version 1.171; Oxford Diffraction Ltd.: Abingdon, UK, 2008.
55. Sheldrick, G.M. A short history of SHELX. *Acta Crystallogr. Sect. A* **2008**, *64*, 112–122. [[CrossRef](#)] [[PubMed](#)]
56. Sheldrick, G.M. Crystal structure refinement with SHELXL. *Acta Crystallogr. Sect. C* **2015**, *71*, 3–8. [[CrossRef](#)] [[PubMed](#)]
57. Farrugia, L.J. WinGX and ORTEP for Windows: An update. *J. Appl. Cryst.* **2012**, *45*, 849–854. [[CrossRef](#)]

58. Macrae, C.F.; Bruno, I.J.; Chisholm, J.A.; Edgington, P.R.; McCabe, P.; Pidcock, E.; Rodriguez-Monge, L.; Taylor, R.; Streek, J.V.; Wood, P.A. Mercury CSD 2.0—New features for the visualization and investigation of crystal structures. *J. Appl. Cryst.* **2008**, *41*, 466–470. [[CrossRef](#)]
59. *Philips X'Pert Data Collector 1.3e*; Philips Analytical B. V.: Almelo, The Netherlands, 2001.
60. *Philips X'Pert Graphic & Identify 1.3e Philips*; Analytical B. V.: Almelo, The Netherlands, 2001.
61. *Philips X'Pert Plus 1.0*; Philips Analytical B. V.: Almelo, The Netherlands, 1999.



© 2017 by the authors. Licensee MDPI, Basel, Switzerland. This article is an open access article distributed under the terms and conditions of the Creative Commons Attribution (CC BY) license (<http://creativecommons.org/licenses/by/4.0/>).